Upcycling of Waste Polyethylene and Cement Kiln Dust to Produce Polymeric Composite Sheets Using Gamma Irradiation

Ehab Khozemy (ehabncrrt2298@yahoo.com)
National Center for Radiation Research and Technology https://orcid.org/0000-0002-4844-9400
Hamdi Radi
National Center for Radiation Research and Technology
Nabila A Mazied
National Center for Radiation Research and Technology

Research Article

Keywords: Recycling, waste plastics, waste rubber, composite, irradiation

Posted Date: December 3rd, 2021

DOI: https://doi.org/10.21203/rs.3.rs-1092910/v1

Abstract

Cement kiln dust (CKD) is a residue produced during the manufacture of cement that contains hazardous solid waste of high toxicity that affects the environment and public health. In this study, the possibility of using cement waste as a filler in the plastic and rubber industry was studied. Different concentrations of (CKD) and gamma irradiation on the mechanical, thermal stability of the prepared composites sheets were investigated. Different concentrations of (CKD) 10, 15, 20, 30, 35, and 40 wt % were prepared with double screw extrusion by mixing waste polyethylene (WPE), de-vulcanized rubber (DWR), and EPDM rubber. These prepared composites were irradiated with doses 25, 50, 75, 100, and 150 kGy to study the effect of radiation on the physical, mechanical properties, and thermal stability of the prepared composite sheets. The prepared composite sheets were characterized and verified by FTIR and soluble fractions. The morphology of the composite sheets was investigated by SEM. Mechanical and thermal properties were investigated to evaluate the possibility of its application in the plastic and rubber industry.

1. Introduction

With the increasing use of polymers, especially plastic and rubber around the world due to its unique characteristics such as tensile strength, flexibility, lightweight, cheapness, and versatility in all aspects of life, whether it is domestic, agricultural, industrial, or even medical, production is increasing in large quantities steadily and hence the amounts of waste polymers generated from consumption also rapidly increased[1, 2]. The negative impact on the environment increases also with the increase of polymer waste, making the recycling of waste polymers is a challenging topic. One of the most common types of these polymers is polyethylene, which with its various types makes up the largest proportion of plastic waste and it is not a biodegradable polymer[3]. The opportunity is good in recycling waste polyethylene due to its nature as thermoplastic polymers. However, repeated recycling of polyethylene causes decreases in molecular weight due to degradation and poor mechanical properties[4], therefore, polyethylene waste prefer to be recycled by mixing with organic or inorganic materials to raise and improve its properties[5, 6].

Rubber tire waste is the most difficult to recycle due to the triple entanglement resulting from the vulcanization process, which makes the recycling process in this case neither possible nor bad because the vulcanized rubber is unable to form new bonds[7]. Therefore, the devulcanization process is necessary for recycling and becomes able to regenerate with new materials to improve their properties and exploit these very large quantities of waste rubber[8]. De-vulcanization of waste tire rubber refers to a process of cleaving the polysulfide bonds crosslinks of vulcanized rubbers[9, 10]. After the devulcanization process not before, the waste rubber can react with new polymers forming new bonds [10–12]. Many studies have been done in this part, including de-vulcanization and blending with different percentages of new polymers to produce a new blend close to the new product in properties that can be used in different applications. (JIANG, Can, et al, 2018) prepared devulcanized waste tire rubber/high-density polyethylene blends by the devulcanization of waste tire rubber with tetraethylenepentamine followed by grafting of HDPE with styrene and glycidyl methacrylate which led to the homogeneity of d-

GTR / HDPE blend and the improvement in the mechanical properties clearly [13]. (Sutanto et al, 2006) studied mixing of reclaimed and devulcanized EPDM with virgin EPDM to enhance and improve the mechanical properties of waste rubber[14]. And since the devulcanized rubber contains a large percentage of carbon, so when re-merging, the process will not need carbon, so a new filler such as cement kiln dust can be added to improve the properties and reduce the cost[15, 16]. Cement kiln dust (CKD) is an inorganic alkaline powder and is not desirable in construction processes because it prevents cement setting and is produced in very large quantities and affects the environment negatively because it is soft, delicate in size, volatile, and difficult to enter into construction operations[17]. And since it contains some elements such as silicon, calcium, iron, and aluminum, which are usually used as a filler in the plastic and rubber industry, the idea was to study the possibility of using cement kiln dust as filler and benefiting from cement dust in this important industry. To benefit from rubber, a process of vulcanization or cross-linking must be carried out, which is carried out using sulfur and various chemical accelerators, which causes great harm to the environment and public health. Therefore, the use of ionizing radiation as an alternative, cheap and easy-to-use technique to obtain a good three-dimensional cross-linking of the rubber through free radicals which formed when the polymer is exposed to ionizing radiation, through which the polymer can combine with the new polymers and form a strong crosslinking with good specifications. In this work, we will study the possibility of making a composite of polyethylene waste with devulcanized waste rubber with the addition of a small portion of new rubber EPDM to increase the compatibility between these polymers and the ease of the mixing process[13] Accompanied by a study of the effect of adding cement dust on the mechanical and thermal properties of composite materials.

2. Materials And Methods

Virgin Ethylene-Propylene-Diene- Monomer (EPDM) commercial trade was obtained from Exxon Chemical Company (Belgium). Waste tire rubber powder (WR) of particle size about 80 meshes produced from the recycled tire was provided by Narobine industries company, Cairo, Egypt. Waste polyethylene (WPE) of transparent bags, was provided by a local supplier, Cairo, Egypt. Cement Kiln Dust (CKD) is a mixture of metal oxides (clay minerals), its composition is listed in (Table 1). Cement dust is produced as an undesired by-product of cement industries, was kindly provided by El-Sweedy cement company, Sues, Egypt, fine powder of particle size about 50 µm. Dioctyl phthalate (DOP) as lubricants oil and compatiplizing agent, Zinc Oxide (ZnO), Lead Oxide (PbO), and Stearic Acid to facilitate and enhancement the plasticity of the compounding process were purchased from Loba-chem (India). Benzoic acid and Hydroquinone for the devulcanization process were purchased from Loba-chem (India). Resin (Rosin) a natural polymer that can interact with the semi-devulcanized rubber and enhance the processability of the milling handle of waste rubber, was provided by a local supplier, Cairo Egypt [9, 18–20].

Table 1
Chemical composition of cement kiln dust (CKD)

Oxides, elements	Ca	Si	Al	Fe	Mg	S	K	Cl
Conc. (%)	52.1	24.5	4.42	3.69	2.06	2.56	6.62	1.36

2.2 De-vulcanization of waste rubber

Is to cleavage the sulfur S-S bonds which crosslink bonds in the vulcanized rubber, totally or partially through chemical interaction under mild milling and temperature around 70 ^{o}C [9]. The Devulcanization process was carried out in both plasticoder (hot mixer) and roll mill. Waste rubber powder (200 gm) is mixed with an adjusted amount of benzoic acid (3%wt) as a proton donator which enhances the cleavage of sulfur bonds into a hot mixer 30 rpm screw speed at 120 ^{o}C for 20 min. the output of extrusion is poured into roll mill at 20 rpm speed and 50 ^{o}C for 20 min., Stearic acid (3%wt) and zinc oxide (2%wt) were added to the mixture to rebuild new bonds between macromolecules with rosin (5%wt) which lead to the capability of devulanized rubbers to interact with new materials[21] and hydroquinone (1%wt) as inhibitor or chain transfer agent interact with sulfur radicals to achieve devulcanization process[19].

2.3 Preparation of formulated samples

Polyethylene was melted in a hot mixer twin-screw with a speed of 80 r/min at 120 ^{o}C for 5 minutes, then, the prepared de-vulcanized waste rubber (DWR), EPDM, and CKD were added for 15 minutes until complete homogeneity of the composite mixture. During the mixing process, laxatives like stearic acid and di-octyl phthalate (DOP) are added to the mixing process. Mixing was continued for 10 min. Various concentrations of (WPE/DWR/EPDM/CKD) Composites are represented in (Table 2). The mixed composite samples are pressed to sheets by Carver hydraulic hot press at 120 ^{o}C for at least 5 minutes and a pressure of 160 kg/cm^{2} on the mold surfaces. The prepared composite sheets were subjected to ^{60}Co-gamma rays at irradiation doses 25, 50, 75, 100, and 150 kGy with a dose rate of ≈1.4 kGy/h.

Table 2
Composition portions of WPE/CKD composite sheets

Sample No.	WPE (gm)	DWR (gm)	EPDM (gm)	CKD (gm)	ZnO (gm)	PbO (gm)	Stearic acid (gm)	DOP (mL)
Blank	120	10	10	-	5	5	3	3
Composite 1	120	10	10	14	5	5	3	3
Composite 2	120	10	10	21	5	5	3	3
Composite 3	120	10	10	28	5	5	3	3
Composite 4	120	10	10	42	5	5	3	3
Composite 5	120	10	10	49	5	5	3	3
Composite 6	120	10	10	63	5	5	3	3

3. Characterizations

3.1 EDX Measurements

Cement Kiln Dust (CKD) analysis was carried out by EDX unit (ISIS Oxford) attached to scanning electron microscopy (Jeol JSM-5400, JEOL, Japan).

3.2 Fourier transform infrared spectroscopy (FTIR)

FTIR studies of WPE, (WPE/DWR/EPDM), and (WPE/DWR/EPDM/CKD) composite samples were recorded on Bruker, Unicom infra-red spectrophotometer, Germany, in the range of 400–4000 $cm^{-}1$.

3.3 Scanning Electron Microscope (SEM)

A scanning electron microscope (SEM) was used to study the morphological structure of the prepared composite sheets using JEOLJSM-5400, Tokyo, Japan.

3.4 Mechanical Measurements

Standard mechanical tests were conducted on dumbbell-shaped specimens of standard width of 4 mm and length of 15 mm. using tensile testing control unit of Hung-Ta Model HT-9112 (Taiwan), load cell capacity 500 kgf, load cell operated 100 kgf, and fitted with an extensometer model HT 8160. The crosshead speed was 500 mm/min.

3.5 Thermogravimetric Analysis measurements

The thermal characteristics of WPE, (WPE/DWR/EPDM) and (WPE/DWR/EPDM)/CKD composite samples have been investigated using Thermogravimetric analysis (TGA) technique with TG-50

instrument Shimadzu; (Japan). This technique was used for the measurements of thermal stability of the samples at a heating rate of 10°C min^{-1}.

3.6 Soluble fraction (SF)

Soluble fraction measurement of the prepared composite sheets was carried out with acetone as a good solvent for rubber, with heating under reflux for 24 h. After extraction, the samples were dried to constant weights in a dry oven at 50 ^{o}C. The soluble Fraction can be calculated as follows:

$$SF = W_0 - W_1 / W_0 \quad (1)$$

Where: W_0 and W_1 represent the dried weight of the sample before and after extraction respectively.

3.7 Swelling

The swelling properties of the prepared samples were studied by placing them (W_1) in a beaker covered with solvent for 24 hours and then weighing again (W_2) and calculating the degree of swelling as follows.

The swelling number (S) is given by:

$$S = W_2 - W_1 / W_1 \quad (2)$$

4. Results And Discussion

4.1 Fourier transform infrared (FT-IR) spectroscopy

Figure 1 shows the FTIR spectra of the WPE, (WPE/DWR/EPDM) blend sample, and (WPE/DWR/EPDM/CKD) composite sheet. FTIR spectrum of WPE (Figure 1a) showed that strong two peaks at 2920 and 2845 cm^{-1} due to C-H stretching vibration mode. The band observed at 1462 and 726 cm^{-1} corresponded to CH_2 bending and rocking respectively, these observed peaks were assigned to PE. For (WPE/DWR/EPDM) blend sample (Figure 1b), a new peak appeared at 2978 cm^{-1} ascribed to aromatic C-H stretching vibration may be due to benzene ring in rosin gum used in devulcanized of DWR. A new peak at 1375 cm^{-1} has also appeared, characteristic of CH_3 bending in polypropylene as the main component of the EPDM rubber used in the blend preparation. For (WPE/DWR/EPDM/CKD) composite sample (Figure 1c), the peak at 2978 cm^{-1} could be masked by the shoulder between 2964- 3008 cm^{-1} due to the addition of CKD. The weak broadband at 3430 cm^{-1} could be assigned hydrogen-bonded to the OH group of silica present in CKD filler.

4.2 Mechanical properties

The blank samples were prepared from 120 gm of WPE, 10 gm (phr) DWR, and 10 gm (phr) of raw EPDM rubber with different concentrations of cement dust (CKD) as filler. Fig. 2 shows the variation of the

tensile strength (TS) as a function of irradiation for the above-mentioned samples. From Fig. 2 it can be seen that the values of TS for all compositions increase with increasing irradiation dose reaching its maximum values at about 100 kGy and after that, the values of TS decrease on increasing the irradiation dose up to 150 kGy. This behavior is due to the increase in the intensity of the crosslinking by increasing the radiation dose and the degradation prevalent at higher doses of radiation where the breakage of the carbon-carbon bond of the main rubber chain may take place at a higher rate than the crosslinking process [22]. Also from Fig. 2, it can be seen that the addition of CKD leads to a relatively increase of TS values (especially at 20 gm (phr) from CKD). The reason for this is due to the large number of interconnections between the composite chains and CKD as a result of the material's characteristics in terms of a small granular size that increases the surface area of diffusion and thus creates a greater amount of synaptic bonds with composite chains.

Figure 3 shows the effect of γ-rays on the elongation at break (E %) of the above-mentioned samples. It can be seen that the E % was increased with irradiation dose up to 25 kGy and then decreased progressively by increasing the filler content (CKD) and irradiation dose up to 150 kGy. This behavior can be explained as by increasing the radiation dose and the filler content, the prepared compound increases crosslinking and the samples relatively harden, which leads to the decrease in the mobility of the molecular chains and thus reduce the elongation properties [23, 24].

4.3 Soluble Fraction and Swelling Number

Figures 4 and 5 show the variation of soluble fraction and number of swelling in acetone as a function of irradiation dose and filler concentrations. The results indicate that by increasing the radiation dose to which the prepared films are exposed, the values of the soluble fraction and swell percentage for all samples gradually decrease. These results are attributed to the difficulty of diffusion of the solvent through the films due to the increased cross-linking that occurred in the samples as a result of exposure to ionizing radiation. We can also see from the figures that the samples treated with cement dust (CKD) filler had a decrease in the percentage of soluble fraction and the number of swelling. This results in less diffusion of the solvent within the material. The same explanation can be given, increase the cross-link density, to reduce the soluble fraction with increasing radiation dose [15].

4.4 Thermal Gravimetric Analysis (TGA)

Thermogravimetric analysis is widely used as a tool to study the degradation of different polymeric materials at a wide range of temperatures. The thermal stability was studied for the blank sample (120 gm of WPE, 10 gm (phr) DWR, and 10 gm (phr) of raw EPDM rubber) and the blank loaded with 20 gm (phr) CKD. All were gamma-irradiated at 100 kGy. Fig. 6 shows the TGA thermograms of the above two formulations. The corresponding rate of thermal decomposition reaction curves for these formulations are shown in Fig. 7. Table 3 shows the weight loss (%) at different heating temperatures and the temperatures of the maximum rate of the thermal decomposition reaction of the above-mentioned formulations.

As shown in Fig. 6, slight differences in the thermal stability between the two formulations based on the remained weight (%) within the temperature range (0 – 300^{0}C) Meanwhile, within the temperature range (350 - 550^{0}C), the blank sample loaded with 20 gm (phr) CKD displayed higher thermal stability than the blank only.

As shown in Fig. 7 and Table 3, the thermal stability in terms of the temperatures of the maximum rate of the thermal decomposition reaction (T_{max}), the blank sample loaded with 20 gm (phr) CKD has T_{max} higher than the blank sample.

Table 3
Weight loss (%) and temperatures of the maximum rate of the thermal decomposition reaction of the prepared composite at different heating temperatures. All samples were gamma-irradiated at 100 kGy.

Sample	Weight loss					T_{max}(^{0}C)
	100^{0}C	200^{0}C	300^{0}C	400^{0}C	500^{0}C	
Blank	0.3	0.5	5	12.9	89.4	470
Composite 3	1.9	2.3	5.6	9.8	74.3	474

4.5 Scanning Electron Microscope (SEM)

SEM images were used to investigate the morphology of the prepared composite sheets. Fig. 8a Illustrates good mixing and complete homogeneity and coherence between the mixed polymers, with no cracks or fracture on the surfaces. Fig. 8b shows the micrograph of the composite after adding filler (CKD) without exposure to radiation, which is evident in the presence of small particles of filler, penetrating the surface of the composite and leading to some cracks and irregularities in the surface. Fig. 8c represented the effect of gamma irradiation on the crosslinking of the composite membranes where the micrograph has been irradiated at 10 Mr. The topographic surface of the composite sheets showed a more compact and homogeneous interlocking shape of one nature without fractures or cracks due to the high degree of crosslinking through the occurrence of successful gamma irradiation and also the small particles of the filler disappeared as if they had melted inside the polymer tissue, which confirms the degree of cohesion that appeared when measuring the tensile strength.

Conclusions

With the increase in human use of plastic and rubber products, waste increases enormously, which makes it affect the environment and heat emissions. Therefore, interest is increasing every day in trying to recycle plastic waste and rubber safely and economically. With the steady increase in construction and cement production, what is known as alkaline cement kiln dust (CKD) is formed as a by-product that is

difficult to use in construction operations, which is a big problem especially for cement producing countries due to its super smoothness and volatility, which is a serious environmental problem. In this research, we succeeded in incorporating cement kiln dust (CKD) as filler in the production of rubber and plastic in large quantities, reaching 40%. For the waste mixing process to be successful, the waste rubber should be recycled through the devulcanization process by thermomechanical methods with the addition of rosin during extrusion to promote the devulcanization process. We succeeded in producing flexible plastic sheets (WPE/DVWR/EPDM) loaded with CKD, have good thermal tolerance and strong tensile properties. The crosslinking was done by exposure to gamma rays. The surface was examined with a microscope, and no cracks or fractures appeared. Mechanical and thermal measurements proved that the cement kiln dust can be used as filler in the production of plastic and rubber industries in a good way.

Declarations

Acknowledgments

All persons who have made significant contributions to the work mentioned in the manuscript (eg, technical assistance, writing and editing assistance, general support) are the working authors and we thank the National Centre of Radiation Research and Technology for the support needed to complete the work

Formatting of funding sources

This research did not receive any specific grant from funding agencies in the public, commercial, or not-for-profit sectors

ORCID

Ehab Khozemy **iD** https://orcid.org/0000-0002-4844-9400

Competing Interests

The authors have no relevant financial or non-financial interests to disclose

Author Contributions

“All authors contributed to the study conception and design. Material preparation, data collection, and analysis were performed by [Ehab E. Khozemy], [Hamdi. Radi] and [Nabila A. mazied]. The first draft of the manuscript was written by [Ehab E. Khozemy] and all authors commented on previous versions of the manuscript. All authors read and approved the final manuscript.”

Conflict of interest: The authors declare that they have no conflict of Interest.

References

1. Fierascu I, Dinu-Pirvu CE, Fierascu RC, Velescu BS, Anuta V, Ortan A, Jinga V. Phytochemical profile and biological activities of *Satureja hortensis* A review of the last decade. Molecules. 2018; *23*(10):2458. https://doi.org/10.3390/molecules23102458
2. Caillet S, Lessard S, Lamoureux G, Lacroix M. Umu test applied for screening natural anti-mutagenic agents. Food Chem. 2011; 124:1699–1707. dOI:1016/j.foodchem.2010.07.082
3. Hamidpour R, Hamidpour S, Hamidpour M, Shahlari M, Sohraby M. Summer savory: From the selection of traditional applications to the novel effect in relief, prevention, and treatment of a number of serious illnesses such as Diabetes, Cardiovascular Disease, Alzheimer's Disease, and Cancer. J Tradit Complement. 2014; 4:140–144.
4. VanZelm E, Zhang Y, Testerink C. Salt tolerance mechanisms of plants. Annu Rev Plant Biol. 2020; 71:403-433. doi:1146/annurev-arplant-050718-100005.
5. Singh P, Arif Y, Siddiqui H, Sami F, Zaidi R, Azam A, Alam P, Hayat S. Nanoparticles enhance the salinity toxicity tolerance in *Linum usitatissiumum* by modulating the antioxidative enzymes, photosynthetic efficiencies, redox status and cellular damage. Ecotoxicol Environ Saf. 2021; 213. doi.org/10.1016/j.ecoenv.2021.112020
6. Vojodi Mehrabani L, Anvari Y, Motallebiazar AR. Foliar application of nano Fe and Se affected the growth and yield of *Pelargonium graveolens* under salinity stress. J Hortic Sci. 2021; 57. doi:22067/JHS.2021.69767.1041.
7. Mehdizadeh L, Moghaddam M, Lakzian A. Alleviating negative effects of salinity stress in summer savory (*Satureja hortensis*) by biochar application. Acta Physiol Plant. 2019; 41(6):doi:10.1007/s11738-019-2900-3.
8. Isayenkov SV, Maathuis FJM. Plant salinity stress: many unanswered questions remain. Front Plant Sci. 2019; http://doi.org/10.3389/fpls.2019.00080.
9. Vojodi Mehrabani L, Valizadeh Kamran R, Hassanpouraghdam MB, Pessarakli M. Zinc sulfate foliar application effects on some physiological characteristics and phenolic and essential oil contents of *Lavandula stoechas* under sodium chloride (NaCl) salinity conditions. Commun Soil Sci Plant Anal. 2017; 48(16):1860-1867. doi:10.1080/00103624.2017.1406105.
10. Rajput VD, Minkina TM, Behal SN, Suskova SN, Mandzhieva S, Singh R, Gorovtsov V, Tsitsuashvili S, Purvis WO, Ghazaryan KA, Movsesyan HS. Effects of zinc-oxide nanoparticles on soil, plants, animals and soil organisms: a review. Environ. Nanotechnol Monit Manag. 2018; 9:76-84. doi:10.1016/j.enmm.2017.12.006
11. Faizan M, Faraz A, Mir AR, Hayat S. Role of zinc oxide nanoparticles in countering negative effects generated by cadmium in *Lycopersicon esculentum*. J Plant Growth Regul. 2020; 1-15. doi:10.1007/soo344-019-10059-2.
12. Moradbeygi H, Jamei R, Heidari R, Darvishzadeh R. Fe_2O_3 nanoparticles induced biochemical responses and expression of genes involved in rosmarinic acid biosynthesis pathway in Moldavian

balm under salinity stress. Physiol Plant. 2020; 169:555-570. doi:10.111/ppl.13077

13. Sheikhalipour S, Esmaielpour B, Behnamian M, Ghohari Gh, Torabi Giglou M, Vachora P, Rastogi A, Brestic M, Skaliy M. Chitosan–Selenium nanoparticle (Cs–Se NP) foliar spray alleviates salt stress in bitter melon. Nanomaterials. 2021; 11:684. https://doi.org/10.3390/nano11030684
14. Kong L, Wang M, Bi D. Selenium modulates the activities of antioxidant enzymes, osmotic homeostasis and promotes the growth of sorrel seedlings under salt stress. Plant Growth Regul. 2005; 45:155–163.
15. Iqbal M, Hussain I, Liaqat H, Ashraf MA, Rasheed R, Rehman AU. Exogenously applied selenium reduces oxidative stress and induces heat tolerance in spring wheat. Plant Physiol Biochem. 2015;94:95–103. https://doi.org/10.1016/j.plaphy.2015.05.012
16. Gupta M, Gupta S. An overview of selenium uptake metabolism and toxicity in plants. Front Plant Sci. 2017; https://doi.org/10.3389/fpls.2016.02074
17. Schmidt W, Thomine S, Buckout TJ. Editorial: Iron nutrition and interactions in plants. Front Plant Sci. 2020; 10. https://doi.Org/10.3389/fpls.2019.01670.
18. Askary M, Telebi SM, Amini F, Dosti Balout Bangan A. Effects of iron nanoparticles on *Mentha piperita* under salinity stress. Biologija. 2017; 63(1): 65-75.
19. Mozafari AA, Ghadakchi Asl A, Ghaderi N. Grape response to salinity stress and role of iron nanoparticle and potassium silicate to mitigate salt-induced damage under in vitro conditions. Physiol Mol Biol Plants. 2018; 24(1):25–35. doi: 10.1007/s12298-017-0488-x.
20. Estaji A, Roosta HR, Rezaei SA, Hosseini SS, Nikham F. Morphological, physiological, and phytochemical response of different *Satureja hortensis* accessions to salinity in a greenhouse experiment. J Appl Res Med Aromat. Plants. 2018; 10:25-33. https://doi.org/10.1016/j.jarmap.2018.04.005
21. Arif Y, Singh H, Siddiqui A, Bajguz A, Hayat S. Salinity induced physiological and biochemical changes in plants: an omics approach towards salt stress tolerance. Plant Physiol Biochem. 2020; 156:64-77. doi: 10.1016/jplaphy.2020.o8.o42
22. Takac T. The relationship of antioxidant enzymes and some physiological parameters in maize during chilling. Plant Soil Environ. 2004; 50:27–32.
23. Subramanyam K, Du Laing G, Van Damme EJM. Sodium selenate treatment using a combination of seed priming and foliar spray alleviates salinity stress in Rice. Front Plant Sci. 2019; 10:116. https://doi.org/10.3389/fpls.2019.00116
24. Jiang C, Zu C, Lu D, Zheng Q, Shen J, Wang H, Li D. Effect of exogenous selenium supply on photosynthesis, Na^+ accumulation and antioxidative capacity of maize (*Zea mays*). Sci Rep. 2017;**7**(1):42039. doi: 10.1038/srep42039
25. Habibi Gh, Sarvary S. The roles of selenium in protecting lemon balm against salt stress. Iran. J Plant Physiol. 2015; 5 (3):1425-1433.

26. Hernandez-Hernandez H, Quiteno-Gutierrez T, Cadenas-Pliego GC, Ortega-Ortiz ZH, Hernandez-Fuentes AD, Fuente MC, Valdes- Reyna J, Juave- Maldonado A. Impact of Selenium and Copper nanoparticles on yield, antioxidant system, and fruit quality of tomato plants. 2019; 8(10):355. https://doi.org/10.3390/plants8100355
27. Lobanov AV, Hatfield DL, Gladyshev VN. Reduced reliance on the trace element selenium during evolution of mammals. Genome Biol. 2008; 9(3). doi:1186/gb-2008-9-3-r62
28. Fathi AR, Zahedi M, Torabian SH, Khoshgoftar AH. Response of wheat genotypes to foliar spray of ZnO and Fe_2O_3 nanoparticles under salt stress. J Plant Nutr. 2017; 40(10):1376-1385. https://doi.org/10.1080/01904167.2016.1262418
29. Soliman ASh, El-Feky SA, Darwish E. Alleviation of salt stress on *Moringa peregrine* using foliar application of Nano fertilizers. J Hortic For. 2015; 7(2):36-47.
30. Pirzad A, Barin M. Iron and Zinc interaction on leaf nutrients and essential oil of *Pimpinella anisum* Iran. J plant physiol. 2018; 8 (4):2507-2515. doi:10.22034/ijpp.2018.543275.
31. Van Raamsdonk JM, Hekimi S. Superoxide dismutase is dispensable for normal animal lifespan. P Natl Acad Sci USA. 2012; 109(15):5785–5790. https://doi.org/10.1073/pnas.1116158109
32. Mathesius U. Flavonoid functions in plants and their interactions with other organisms. Plants. 2018; 7(2):30. https://doi.org/10.3390/plants7020030.
33. Tan J, Zhao H, Hong J, Han Y, Li H, Zhao W. Effects of exogenous nitric oxide on photosynthesis, antioxidant capacity and proline accumulation in wheat seedlings subjected to osmotic stress. World J Agric Sci. 2008; 4(3):307–313.
34. Hassanpouraghdam MB, Vojodi Mehrabani L, Tzortzakis N. Foliar application of Nano-Zinc and Iron affects physiological attributes of *Rosmarinus officinalis* and quietens NaCl salinity depression. J soil Sci Plant Nutr. 2019; 20(2):335-345. Doi:10.1007/42729-019-00111-1.
35. Kanjana D. Foliar study on effect of iron oxide nanoparticles as an alternate source of iron fertilizer to cotton. Int J Chem Stud. 2019; 7(3):4374-4379.
36. Bakhtiari M, Moaveni P, Sani B. The effect of Iron nanoparticles spraying time and concentration on wheat. Biological forum Int J. 2015; 7(1):679-683.
37. Karimi M, De Meyer B, Hilson P. Modular cloning in plant cells. Trends in plants Sci. 2005; 10(3):103-105. https://doi.org/10.1016/j.tplants.2005.01.008
38. Do Nascimento da silva E, Cidade M, Heerdt G, Ribessi RL, Morgon NH, Cadore S. Effect of selenite and selenite application on mineral composition of lettuce plants cultivated under hydroponic conditions: Nutritional balance overview using multifaceted study. J Braz Chem Soc. 2017; 29(2). https://doi.org/10.21577/0103-5053.20170150.
39. Marco Del Pino A, Guiducci M, Aamato R, Di Michele A, Tosti G, Datti A, Alberto Palmerini C. Selenium maintains cytosolic Ca^{2+}homeostasis and preserves germination rates of maize pollen under H_2O_2-induced oxidative stress. Sci Rep. 2019; 9 (1):1-9. doi:1038/s41598-019-49760-3

40. Michard E, Alves F, Feijo JA. The role of ion fluxes in polarized cell growth and morphogenesis: the pollen tube as an experimental paradigm. Int J Dev Biol. 2008; 53(8-10):1609–1622. doi:1387/ijdb.072296em
41. Hancock JT, Desikan R, Neill SI. Role of reactive oxygen species in cell signaling pathways. Biochem Soc Trans. 2001; 29(2):345–350. doi:1042/BST0290345
42. Steinhorst L, Kudla J. Calcium - a central regulator of pollen germination and tube growth. Biochim Biophy Acta. 2013; 1833(7):1573–1581.
43. Ursache-Oprisan M, Focanici E, Creanga D, Caltun OF. Sunflower chlorophyll levels after magnetic nanoparticle supply. Afr J Biotechnol. 2011; 10(36):7092-7098.
44. Camel V. Solid phase extraction of trace elements. Spectrochim Acta Part B. 2003; 58:1177-1233.
45. Prochazkova D, Sairam RK, Srivastava GC, Singh DV. Oxidative stress and antioxidant activity as the basis of senescence in maize leaves. Plant Sci. 2001; 161(4):765–771.
46. Chrysargyris A, Drouza C, Tzortzakis N. Optimization of potassium fertilization/nutrition for growth, physiological development, essential oil composition and antioxidant activity of *Lavandula angustifolia* J Soil Sci Plant Nutr. 2017; 17(2):291–306. doi: 10.4067/S0718-95162017005000023
47. Honarjoo N, Hajrasuliha Sh, Amini H. Comparing three plants in absorption of ions from different natural saline and sodic soils. Int J Agri Crop Sci. 2013; 6(14):988–993.
48. Fedina I, Georgieva K, Velitchkova M, Grigorova I. Effect of pretreatment of barley seedlings with different salts on the level of UV-B induced and UV-B absorbing compounds. Environ Exper Bot. 2006; 56:225-230. doi:1001016/J.ENVEXPBOT. 2005.02.006.
49. Nareshkumar A, Veeranagamallaiah G, Pandurangaiah M, Kiranmai K, Amaranathareddy V, Lokesh U, Venkatesh B, Sudhakar C. Pb-stress induced oxidative stress caused alterations in antioxidant efficacy in two groundnuts (*Arachis hypogaea*, L.) cultivars. Agric Sci. 2015; 6 (10):1283-1297. doi: 4236/as.2015.610123.
50. Sairam RK, Rao KV, Srivastava GC. Differential response of wheat genotypes to long-term salinity stress in relation to oxidative stress, antioxidant activity and osmolyte concentration. Plant Sci. 2002; 163(5):1037-1046. https://doi.org/10.1016/S0168-9452(02)00278-9.
51. Quettier-Deleu C, Gressier B, Vasseur J, Dine T, Brunet C, Luyckx M, Cazin M, Cazin JC, Bailleul F, Trotin F. Phenolic compounds and antioxidant activities of buckwheat (*Fagopyrum esculentum* moench) hulls and flour. J Ethnopharmacol. 2000; 72 (1–2):35–42. doi: 10.1016/S0378-8741(00)00196-3.
52. Kim KH, Tsao R, Yang R, Cui SW. Phenolic acid profiles and antioxidant activities of wheat bran extracts and the effect of hydrolysis conditions. Food Chem. 2006; 95 (3):466-473. doi: 10.1016/j.foodchem.2005.01.032.
53. Rios-Gonzalez K, Erdei L, Lips SH. The activity of antioxidant enzymes in maize and sunflower seedlings as affected by salinity and different nitrogen sources. Plant Sci. 2002; 162(6):923-930. https://doi.org/10.1016/S0168-9452(02)00040-7.

Figures

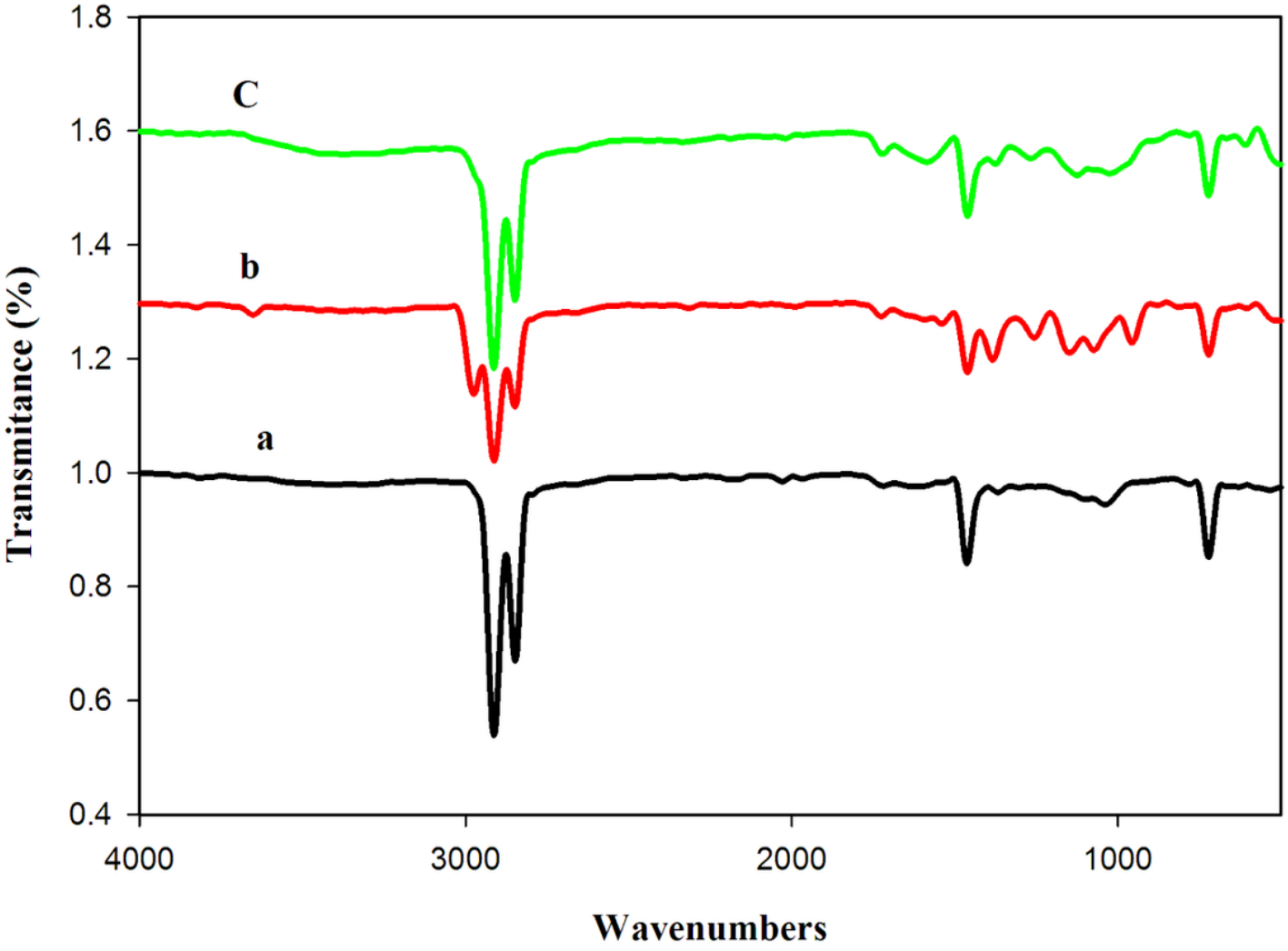

Figure 1

FTIR spectra of (a) WPE, (b) (WPE/DWR/EPDM) blend (c) (WPE/DWR/EPDM/CKD) composite.

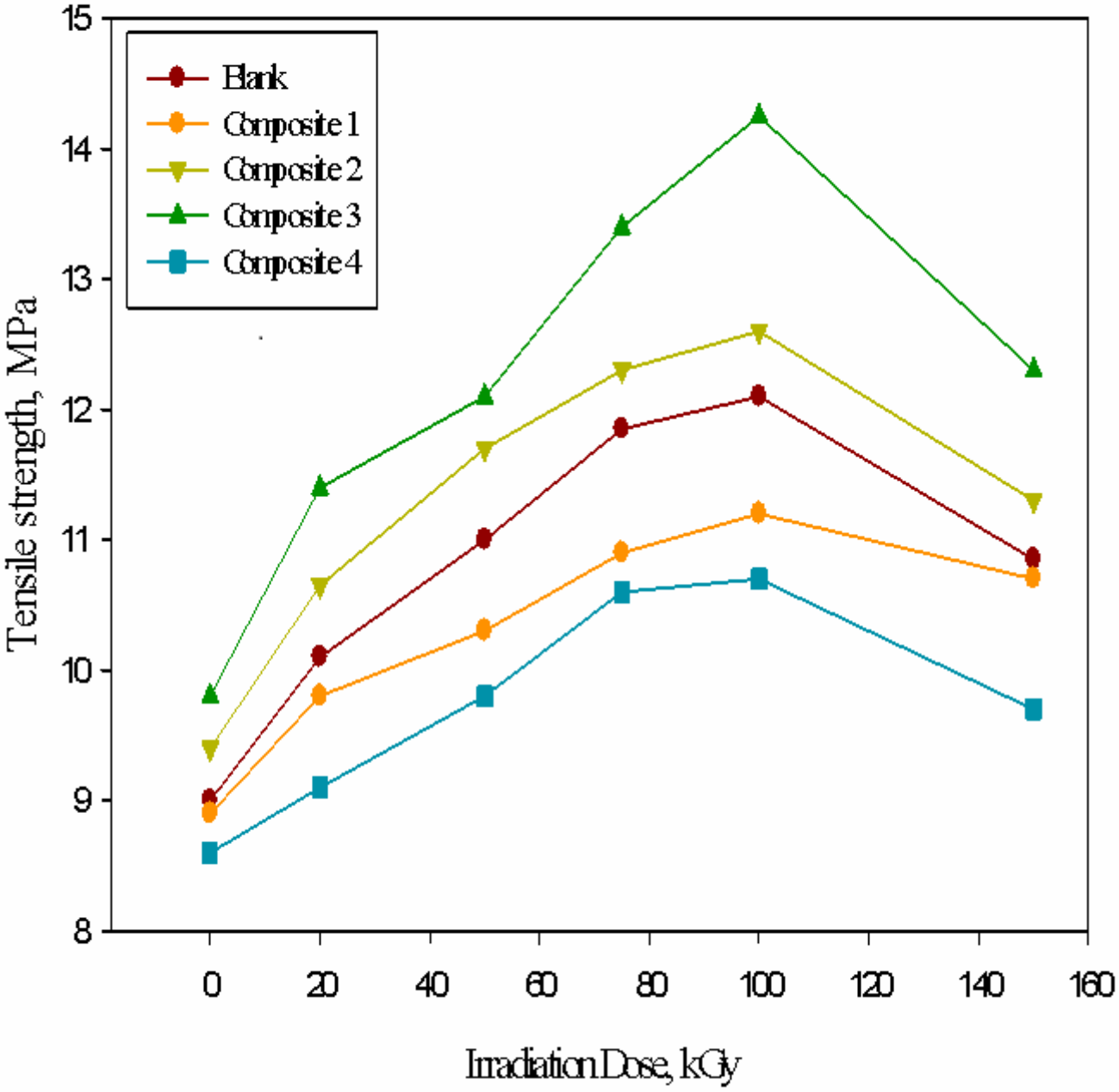

Figure 2

Tensile strength of (WPE/DWR/EPDM) sheets and with loaded with different concentrations of CKD as a function of irradiation dose

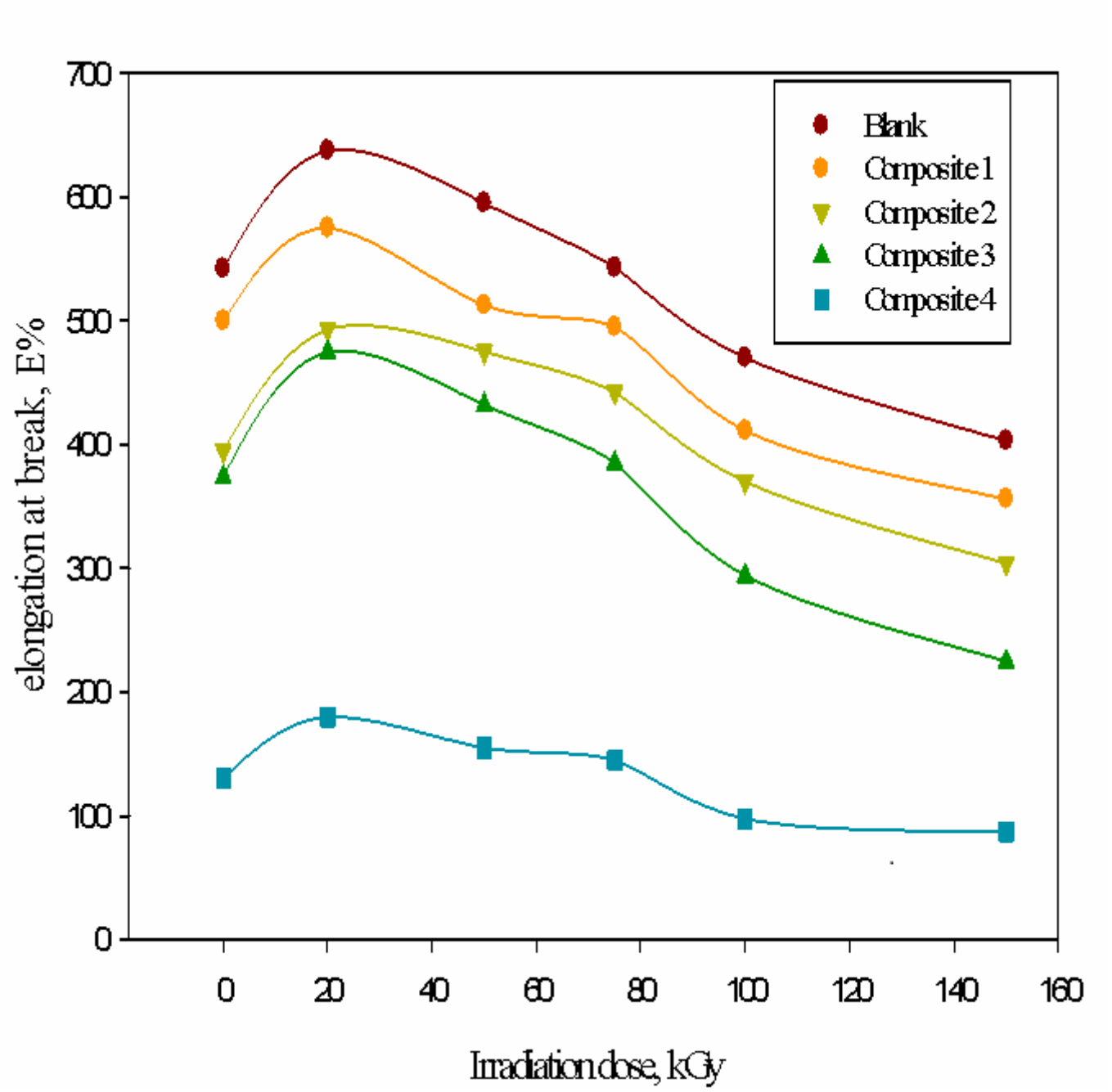

Figure 3

Elongation at break of (WPE/DWR/EPDM) sheets and with loaded with different concentrations of CKD as a function of irradiation dose

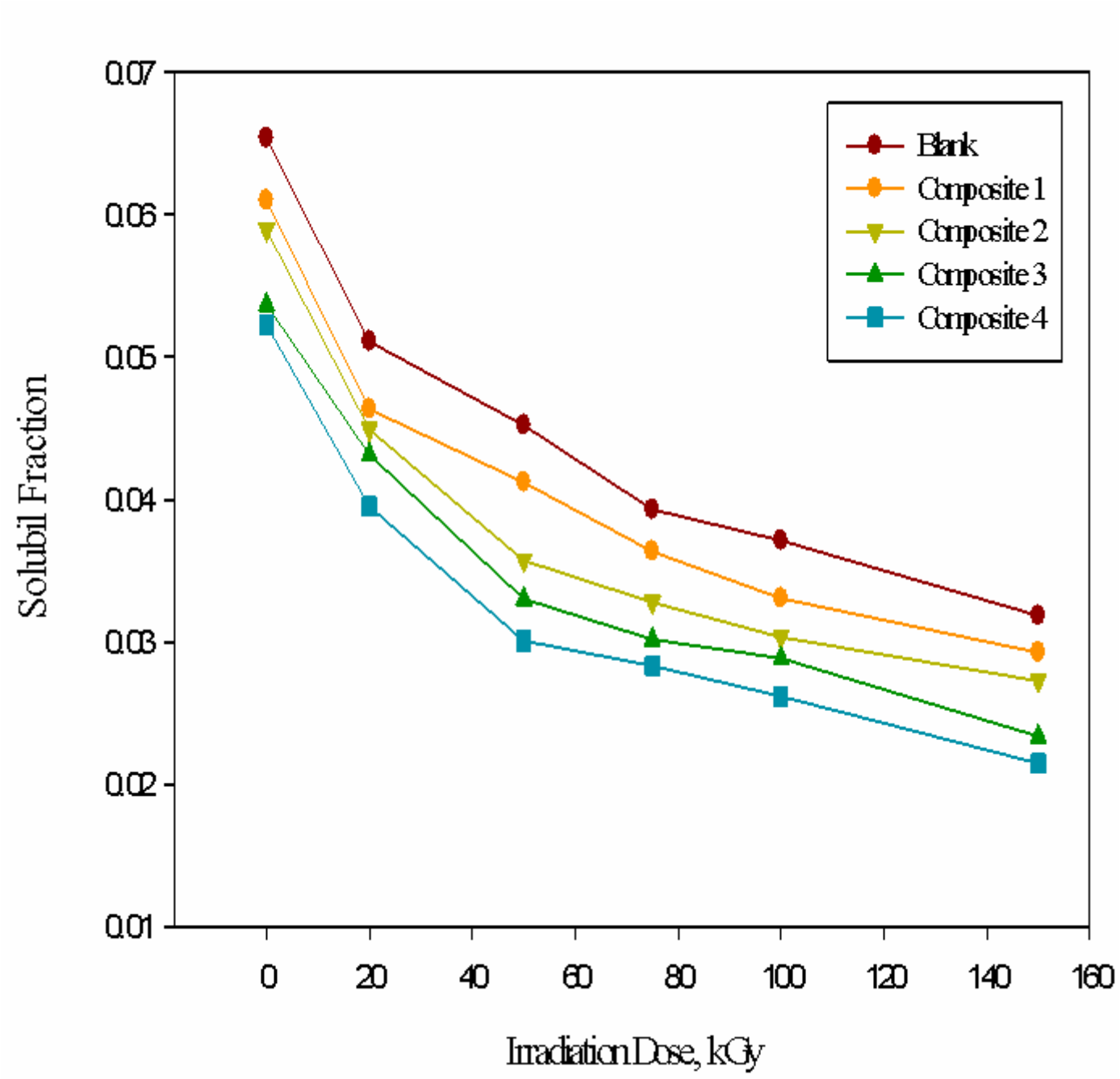

Figure 4

Soluble fraction of (WPE/DWR/EPDM) composite sheets and with loaded with different concentrations of CKD as a function of irradiation dose

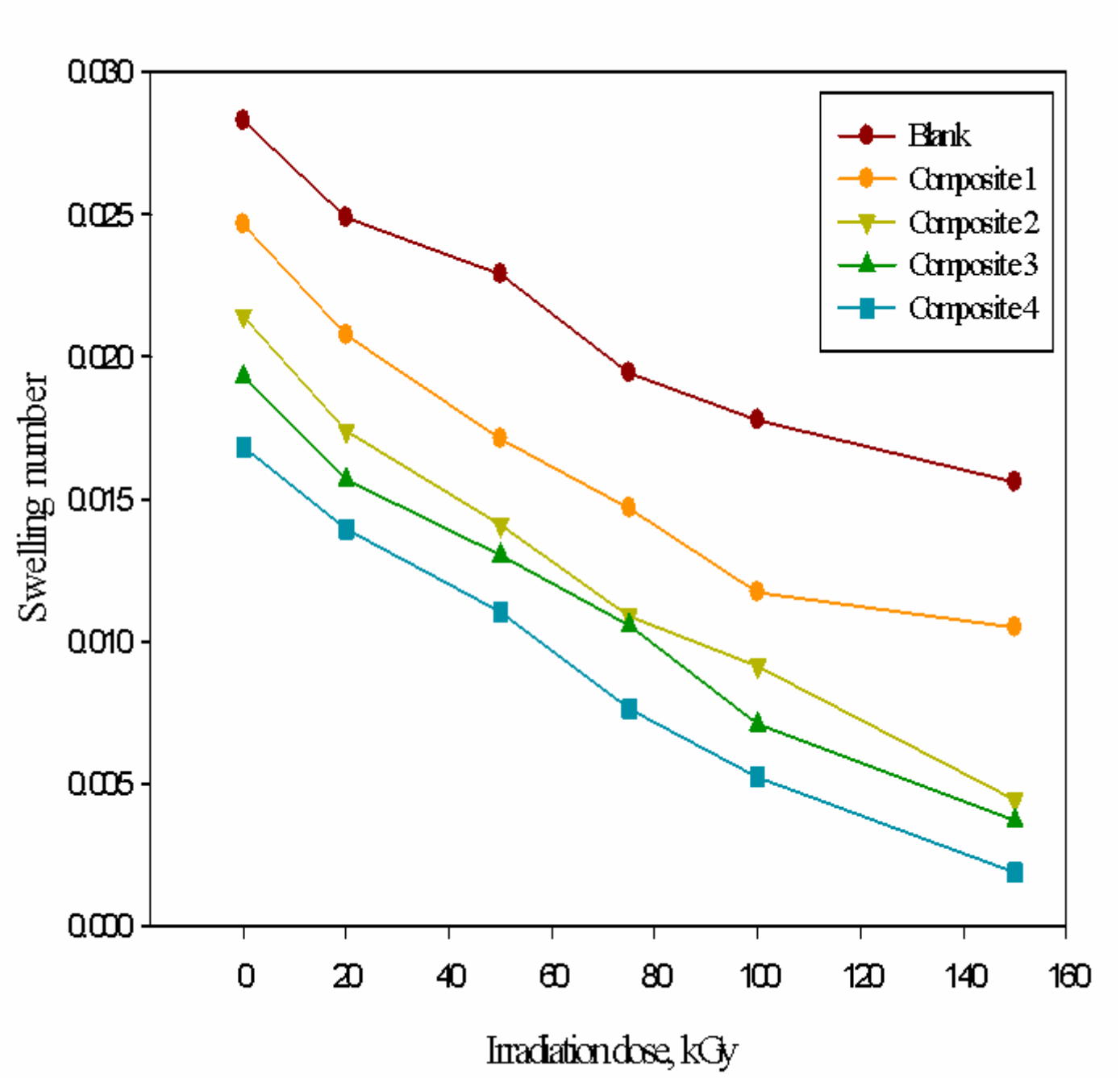

Figure 5

swelling number of (WPE/DWR/EPDM) composite sheets and with loaded with different concentrations of CKD as a function of irradiation dose

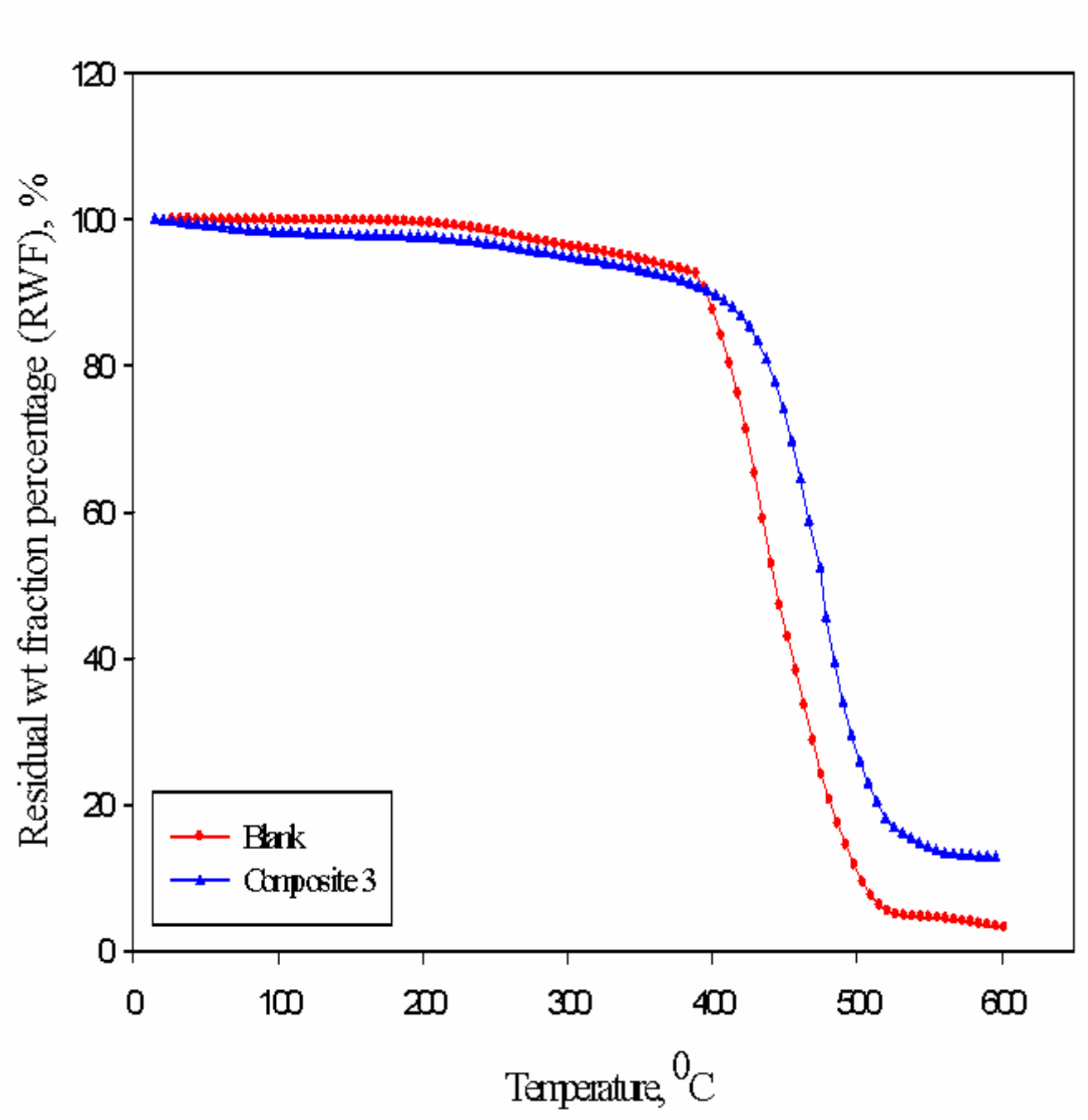

Figure 6

Residual weight fraction percentage against the temperature of the composite sheets irradiated at 100 kGy

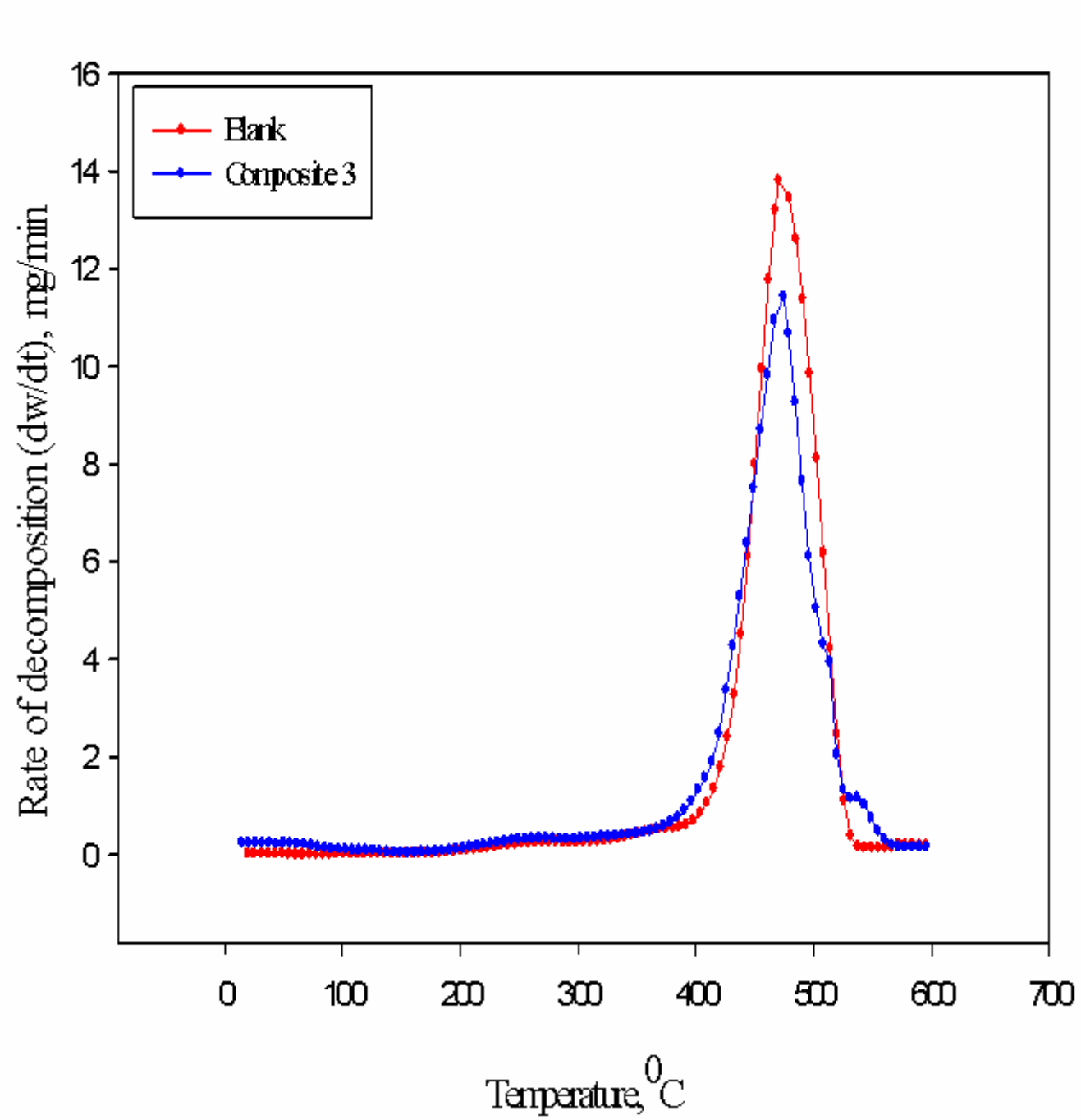

Figure 7

Rate of decomposition against the temperature of the composite sheet irradiated at 100 kGy

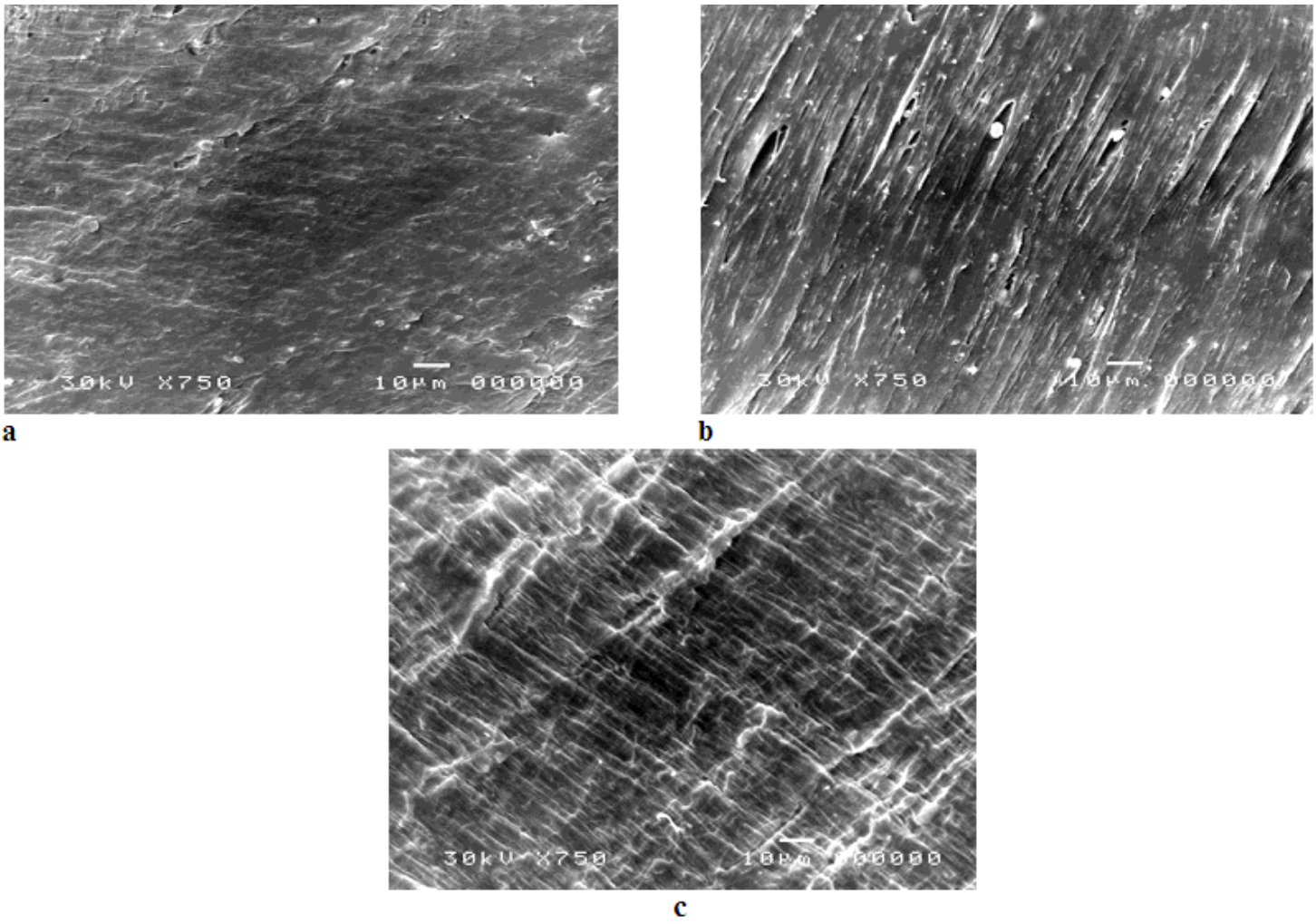

Figure 8

Scanning electron micrograph of (a) (WPE/DWR/EPDM), (b) un-irradiated (WPE/DWR/EPDM)/CKD and (C) irradiated (WPE/DWR/EPDM)/CKD at 100 kGy